Reaction-enhanced permeability during serpentinite dehydration

Eric Tenthorey
Research School of Earth Sciences, Australian National University, Canberra ACT 0200, Australia
Stephen F. Cox
Research School of Earth Sciences and Department of Geology, Australian National University, Canberra ACT 0200, Australia

ABSTRACT

Fluid mobilization during prograde metamorphic reactions is a poorly understood, yet crucial, phenomenon that has implications for a number of geologic problems. Here we present the first experiments to characterize permeability evolution during dehydration of a natural rock. Dehydration of serpentinite specimens resulted in the generation of pore space and the rapid development of an interconnected pore network. During breakdown of antigorite to olivine + talc + H_2O, permeability increased rapidly by at least three orders of magnitude. In natural systems, such an increase in permeability would be transitory, because high confining stresses would rapidly eliminate the porosity generated during reaction. Such transitory, reaction-enhanced permeability of serpentinite provides a mechanism by which fluids can migrate and possibly facilitate subduction-zone seismicity and contribute to partial melting of the mantle wedge. The results presented also have implications regarding middle- to deep-crustal fluid flow.

Keywords: permeability, dehydration reactions, serpentinite, fluid migration, subduction zones.

INTRODUCTION

Prograde metamorphic reactions within Earth's lithosphere can cause profound changes in a rock's physical and rheological properties. One important subset of reactions is dehydration reactions, such as the breakdown of chlorite, micas, amphiboles, and serpentine, that release large amounts of water while decreasing the solid volume and possibly generating pore space and associated rock permeability. Fluids originating from such reactions are thought to be the cause of melting and magma generation in certain tectonic regimes such as subduction zones (Ulmer, 2001) and might also metasomatize parts of the crust, possibly forming economic mineral deposits. It has also been suggested that fluids released from dehydration reactions can lead to the development of fluid pressures in excess of hydrostatic if the permeability of surrounding rocks is low enough to prevent fluid drainage (e.g., Etheridge et al., 1984). Such a reduction of effective confining pressure associated with dehydration reactions may also cause nucleation of earthquakes within subducting slabs (Davies, 1999; Kirby et al., 1996).

The chemical and physical interaction between fluids and rock depends greatly on the permeability evolution of the dehydrating system. Permeability is the key factor that will determine whether released fluids migrate continuously through a porous network or build up high fluid pressure and induce brittle failure, forming the high-permeability pathways through which episodic flow occurs (Cox, 1999; Manning and Ingebritsen, 1999; Wong et al., 1997). Considering the importance of metamorphic fluids to a wide range of geologic problems, very little work has been done to understand the hydraulic behavior that accompanies mineral dehydration. Most experimental studies have focused on strength variations caused by dehydration (Ko et al., 1997; Meade and Jeanloz, 1991; Murrell and Ismail, 1976; Raleigh and Paterson, 1965) or on reaction progress and fluid expulsion as a function of boundary conditions (i.e., drained vs. undrained) (Ko et al., 1997; Miller et al., 2003). Zhang et al. (2000) examined permeability evolution in a synthetic quartz + calcite system undergoing decarbonation and observed that high specimen permeabilities were maintained because of the reaction. Similarly, by using a natural amphibolite, Zharikov et al. (2000) showed that the onset of dehydration was associated with an increase in permeability although the hydraulic evolution was not characterized. Here we present the first experimental results showing how permeability evolves during dehydration of natural serpentinite.

In this study we examine permeability evolution during active dehydration of cores of natural serpentinite. We conducted both isostatic experiments and experiments in which a significant differential stress was applied to the sample; accordingly, a wide range of stress conditions was examined. In early experiments (Murrell and Ismail, 1976; Raleigh and Paterson, 1965), strength tests on partially dehydrated serpentinite specimens showed that dehydration reactions had an important weakening effect, presumably due to trapped pore fluids that reduced the effective confining pressure and a loss of cohesive strength due to structural changes. In view of these results, dehydration under conditions of differential stress might be expected to result in fluid pressure–induced shear failure in which highly permeable pathways are localized within the sheared zone. Such a process would differ greatly from the isostatic case, where reaction-induced dilatant cracks would be randomly oriented, distributing the damage zone and associated permeable pathways throughout the sample.

The main reaction of interest is the initial breakdown of serpentine under low-pressure conditions (Ulmer and Trommsdorff, 1995),

$$\text{antigorite} = 18\text{olivine} + 4\text{talc} + 27H_2O, \qquad (1)$$

which involves a 24% reduction in solid volume. At pore-fluid pressure (P_p) = 50 MPa, the equilibrium boundary for this reaction is between 500 and 550 °C.

Lower-temperature reactions also occur, involving the reaction of serpentine with accessory magnesite or dolomite to yield olivine, diopside, and volatiles:

$$\text{antigorite} + 20\text{magnesite} = 34\text{olivine} + 20CO_2 + 31H_2O \qquad (2)$$

and

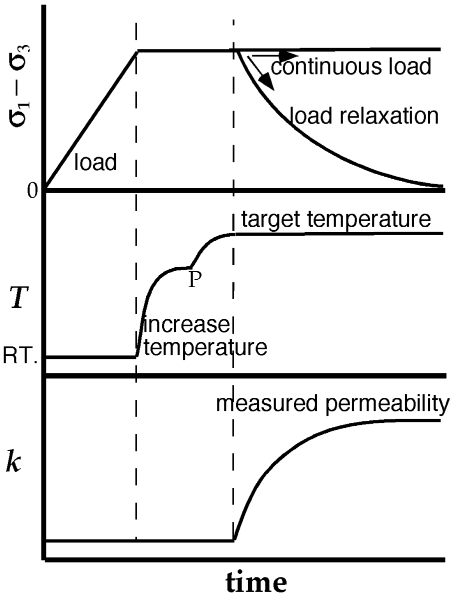

Figure 1. Schematic illustration showing evolution of differential stress ($\sigma_1 - \sigma_3$), temperature (*T*), and permeability (*k*) during a typical experiment. Time axis begins after 100 MPa confining pressure and 50 MPa pore pressure have been applied to specimen. After load has been applied, temperature is first allowed to stabilize at 500 °C (point P) to ensure that specimen and jacket are perfectly coupled. When target temperature has been reached, load may be either allowed to relax or maintained at a constant level. In both cases a significant increase in permeability is observed. RT.—room temperature.

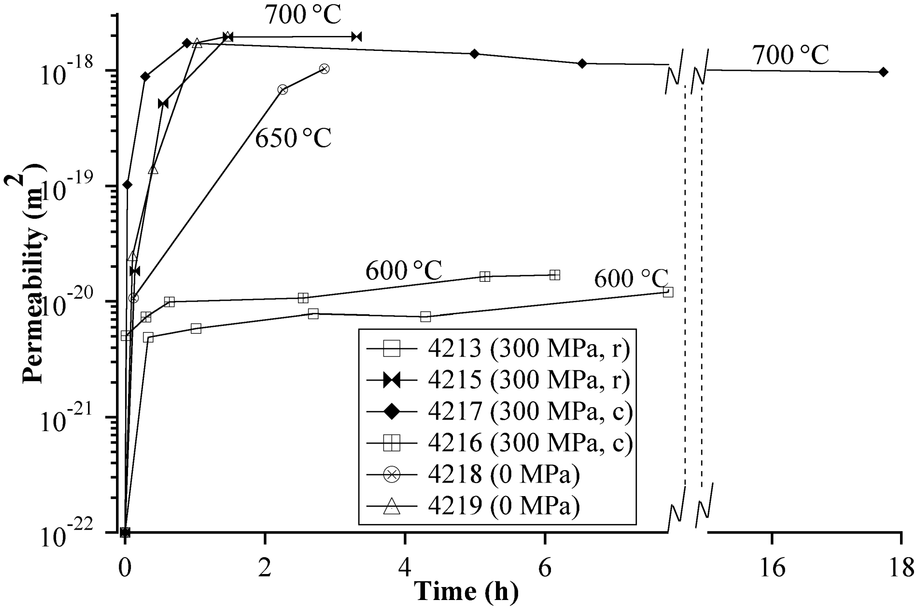

Figure 2. Permeability-evolution curves for dehydrating serpentinite specimens. Initial permeability is assumed to be 1 × 10^{-22} m^2. In legend, numbers within parentheses represent differential stress: r—relaxed stress conditions; c—stress maintained continuously on specimen as reaction progresses. Total breakdown of antigorite to olivine + talc results in permeability increase to ~1 × 10^{-18} m^2.

$$\text{antigorite} + 5\text{dolomite} = 24\text{olivine} + 5\text{diopside} + 10CO_2 + 31H_2O. \quad (3)$$

At $P_p = 50$ MPa and low mole fractions of CO_2 ($X_{CO_2} = 0.1$), these two reactions occur at ~450 °C (Trommsdorff and Evans, 1977) and result in a solid volume decrease of 36% and 33%, respectively.

EXPERIMENTAL METHODOLOGY

The starting material used in the experiments is a fine-grained, mesh-textured serpentinite possessing no visible porosity. The cores of serpentinite measure 1 cm (diameter) by 2.2 cm (length) and contain ~90% antigorite, 5% dolomite, and 5% magnesite by volume. Dolomite and magnesite occur mainly as isolated aggregates within the serpentine matrix. Mineral phases before and after dehydration were determined by X-ray diffractometry and energy- and wavelength-dispersive spectrometry. Scanning electron microscopy (SEM) was used to characterize the microstructure of run products.

All experiments were conducted in a Paterson gas apparatus capable of independently controlling confining pressure (P_c), pore-fluid pressure, differential stress, and strain rate ($d\varepsilon/dt$). For a detailed description of the specimen and vessel configuration, see Zhang et al. (1994). During each experiment, P_c and P_p were first raised to 100 MPa and 50 MPa, respectively. The specimens were then shortened axially at a nominal $d\varepsilon/dt = 1.8 \times 10^{-5}$ s^{-1} until the target differential stress was reached, at which time deformation was stopped. Temperature was then increased to target levels ranging from 600 to 700 °C, after which permeability measurements commenced (Fig. 1). Upon the onset of reaction, differential stress was allowed to decay in response to the solid volume decrease, except in a couple of experiments, where a continuous differential stress was maintained on the sample by further straining the specimen.

Permeability measurements were made by using the steady-state flow method, which consists of imposing a known pore-pressure gradient across the specimen and measuring the resultant flow rate, which is proportional to permeability.[1]

RESULTS

Physical Behavior

In all experiments, fluid-expulsion rate is most rapid immediately after the target temperature is reached and levels off with time. The highest temperature experiments are characterized by expulsion rates of ~0.6 mm^3/s at the earliest stages. This behavior is markedly different from that seen in previous dehydration experiments on gypsum, which exhibited an early period of slow fluid expulsion (Ko et al., 1997), although enhanced expulsion was observed under triaxial conditions. The total volume of fluid released increases greatly between 600 °C and 700 °C. In all cases, the fluid-expulsion rate evolves in a manner very similar to that of permeability, the evolution of which is shown in Figure 2. All experiments exhibit a significant permeability increase during reaction; the largest change occurs at temperatures above 650 °C. As with the fluid-expulsion data, the rate of permeability change is greatest in the early stages of reaction and levels off once fluid expulsion ceases. At 600 °C, permeability increases by at least one order of magnitude and levels off at ~10^{-20} m^2 after 3 or 4 h of reaction. By contrast, for experiments conducted at 650 °C and 700 °C, permeability increases to ~10^{-18} m^2. In the longest experiment, conducted at 700 °C, permeability increases to an early peak permeability of 1.7 × 10^{-18} m^2 before dropping slowly to 9.7 × 10^{-19} m^2 after ~1 day of reaction. Experiments conducted at the same temperature, with either variable differential stress, or isostatic stress states, have a very similar permeability evolution.

Once temperature has been reached and reaction initiated, any differential stress applied to the specimen is observed to decrease with time. The rate of decrease is most rapid in the

---

[1] GSA Data Repository item 2003132, a detailed description of the permeability measurement technique, is available online at www.geosociety.org/pubs/ft2003.htm or on request from editing@geosociety.org or Documents Secretary, GSA, P.O. Box 9140, Boulder, CO 80301-9140, USA.

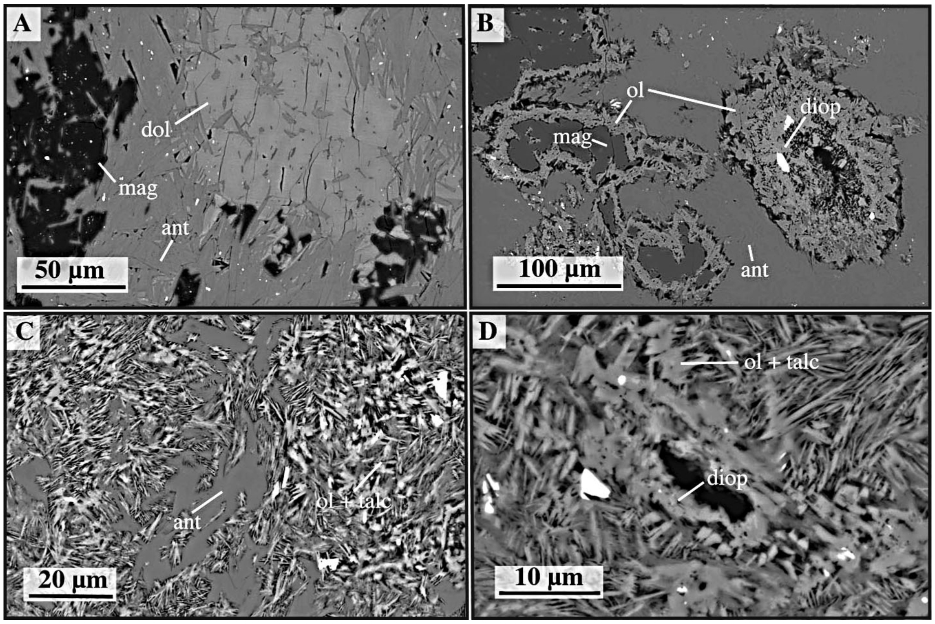

Figure 3. Scanning electron micrographs of starting serpentinite and reaction products after dehydration reactions. A: Starting serpentinite specimen with pods of dolomite (dol) and magnesite (mag) within matrix of antigorite (ant). B: Experiment at 600 °C showing coronal reaction textures between magnesite, dolomite (reacted out), and antigorite resulting in olivine (ol) and diopside (diop). C: Experiment at 650 °C showing partial breakdown of antigorite to olivine + talc. Reaction products exhibit fibrous, interwoven texture in which individual olivine and talc grains are difficult to discern. D: High-magnification image of complete antigorite breakdown at 700 °C. Diopside corona texture is preserved from lower-temperature reaction of antigorite with dolomite. Bright spots in images are Fe-sulfide.

early stages and levels off as reaction proceeds. The total load relaxation depends on temperature; the differential stress drops to 0 over a period of 1–2 h at 700 °C. Load relaxation occurs in response to the solid-volume decrease associated with dehydration and is extracted from the corresponding axial-displacement data. It is important to note in Figure 2 that the differential stress on the specimen has little effect on permeability evolution during reaction.

Microstructure

Experiments conducted at 600 °C are characterized by initial reaction between antigorite and the two carbonates magnesite and dolomite. Reaction between serpentine and the two carbonates is characterized by corona textures in which remnant carbonate domains are sometimes preserved (Fig. 3). Carbonate reactions 2 and 3 generate considerable porosity within the reaction zone and also induce micrometer-scale cracking in the surrounding antigorite. Narrow cracks appear to connect separate reaction zones and may be conduits for fluid flow through the sample. The porosity generated in the corona reaction zones may also be interconnected in three dimensions and therefore might also be a source of increased permeability.

In all the experiments conducted above 600 °C, primary antigorite has reacted partially or completely to olivine and talc. The secondary products appear as an interwoven, fibrous mosaic; individual olivine and talc grains are difficult to distinguish by using SEM. Expected porosity for the antigorite breakdown reaction is 24%, under the assumptions of no concurrent deformation and no physical compaction. SEM images of the run products (Figs. 3C, 3D) show that experimental specimens possess porosity values that are consistent with expectations if some compaction during dehydration is assumed. This intergranular porosity between olivine and talc grains is the likely cause of the elevated permeabilities in the higher-temperature experiments.

DISCUSSION AND IMPLICATIONS

This paper describes the first-ever set of experiments characterizing permeability evolution of an actively dehydrating serpentinite. The results just presented show that dehydration of serpentinite leads to a large transitory increase in porosity and permeability, an observation that has profound implications for naturally dehydrating systems in subducting slabs and in middle- to lower-crustal metamorphic regimes. Although our experiments were not conducted at the high pressures typical of the basal crust or subduction zones, the effective stress on the specimens was greater, because natural systems are expected to have near-lithostatic fluid pressures during devolatilization reactions (Etheridge et al., 1984). Our initial hypothesis was that dehydration of a highly impermeable serpentinite during active deformation would result in fluid-assisted shear failure due to a reduction in the effective stress. However, it appears that an interconnected pore network rapidly developed, allowing pore fluid to drain from the sample and maintain initial effective-stress conditions. The fact that fluid was allowed to drain from the specimens makes our experiments different from those of most other studies, where pore fluid was trapped and pore pressures were forced to increase (Dobson et al., 2002; Raleigh and Paterson, 1965).

In natural systems, the elevated permeabilities observed during dehydration would only be a transitory characteristic. As dehydration progresses to completion and all fluids are expelled from the rock, the pore structure would collapse owing to brittle failure or creep. The time scale on which such porosity destruction would occur depends on the relative kinetics of dehydration and deformation (Balashov and Yardley, 1998). This effect can be observed in experiment 4217 (Fig. 2), where after reaching a peak at the early stages, permeability then gradually drops by ~50%. The collapse in pore space associated with fluid drainage is also indicated by the large to complete relief of the imposed differential stress in the relaxed experiments. In Figure 2 it can be seen that the applied differential stress imposed on the experimental specimens had no discernible effect on permeability evolution, nor did continuous or relaxed differential stress conditions have any effect.

One of the interesting implications of our results pertains to the origin of lower seismic planes for intermediate-depth earthquakes in subduction zones, which usually extend down to 200 km depth. Although the upper planes may be a result of dehydration reactions in the basaltic crust of the slab (Kirby et al., 1996), subsequent work suggests that the lower planes are related to the dehydration of serpentinized oceanic mantle (Dobson et al., 2002; Peacock, 2001), although other models have also been proposed. Serpentinization of mantle peridotites is thought to occur when fluids permeate down large oceanic transform faults or normal faults at the outer rise. As subduction proceeds, fluids released during the breakdown of antigorite are thought to nucleate earthquakes through elevated pore pressures, which cause fluid-assisted shear failure or weaken preexisting fault features. However, the mobility of fluids released during subduction has long been an unknown parameter owing to the lack of any permeability data, and therefore the models involving fluid-assisted earthquake nucleation are highly speculative. The observation that lower-plane, intermediate-depth earthquakes are double-couple events, with no volume collapse or hydrofracture components (Dobson et al., 2002), also leads to some confusion regarding the exact mechanism of earthquake nucleation. Peacock (2001) constructed a thermal model for subduction in northeastern Japan that suggests that lower-plane seismic events occur at lower temperatures with increasing depth. This model suggests that earthquake nucleation is closely linked to a reaction with negative Clapeyron slope and a total decrease in volume during dehydration. However, any model directly invoking these volume changes to nucleate earthquakes is inconsistent with the double-couple seismic signatures.

To reconcile these problems, we propose a model that is consistent with both previous observations and the results presented in this study. On the basis of pressure-temperature considerations and the observed negative Clapeyron slope, the likely antigorite reaction relevant to lower seismic planes is antigorite's breakdown to enstatite + olivine + H_2O. Although we have reported permeability results for antigorite's lower-pressure breakdown to olivine + talc + H_2O ($dP/dT > 0$), both these reactions result in a decrease in solid volume and will likely generate transiently interconnected porosity. In fact, the higher-pressure breakdown to olivine + enstatite results in a greater reduction in solid volume; the reaction products are less compressible than olivine + talc and therefore might be even more efficient in generating a permeable pore network. As dehydration progresses, we envisage that fluids are squeezed from the porous network owing to surrounding stresses and migrate to weak or previously faulted zones within the slab. Because of the potentially high fluid fluxes involved, high pore-fluid pressures can rapidly build up in such zones, decreasing frictional resistance, which eventually leads to rupture and generation of a double-couple seismic event. Such a model is consistent with previous work indicating that failure occurs on reactivated faults initially generated at the outer rise (Jiao et al., 2000). Furthermore, the interface between serpentinized domains and unserpentinized peridotites is likely to be a zone of high stress while compaction occurs in the dehydrating section. Immediately following rupture events, permeability in the fault plane is expected to be very high, providing a mechanism by which fluids may eventually migrate upward and contribute to partial melting in the overlying mantle wedge.

The results from this study also have implications for fluid transport during dehydration reactions in the middle to deep crust. Although the deep crust has been viewed as a ductile-deforming, impermeable horizon, a number of geochemical studies have pointed to large fluid fluxes to depths as great as 40 km (Jamtveit et al., 2000; McCulloch and Woodhead, 1993; Roering et al., 1995). Such transiently elevated permeability is expected in the middle to lower crust during active deformation (Zhang et al., 1994), while low permeabilities would be favored at other times. Reaction-enhanced permeability during dehydration reactions provides a potentially important mechanism by which deep-seated fluids transiently become highly mobile during metamorphism (Ferry, 1994).

ACKNOWLEDGMENTS

Many thanks to J. Hermann and R. Kerr for discussion and advice. We also thank C. Saint and H. Kokkonen for technical assistance. Reviews by J. Ferry and T.-F. Wong greatly improved the paper.

REFERENCES CITED

Balashov, V.N., and Yardley, B.W.D., 1998, Modelling metamorphic fluid flow with reaction-compaction-permeability feedbacks: American Journal of Science, v. 298, p. 441–470.

Cox, S.F., 1999, Deformational controls on the dynamics of fluid flow in mesothermal gold systems, *in* McCaffrey, K.J.W., et al., eds., Fractures, fluid flow and mineralization: Geological Society [London] Special Publication 155, p. 123–140.

Davies, J.H., 1999, The role of hydraulic fractures and intermediate-depth earthquakes in generating subduction-zone magmatism: Nature, v. 398, p. 142–145.

Dobson, D.P., Meredith, P.G., and Boon, S.A., 2002, Simulation of subduction zone seismicity by dehydration of serpentine: Science, v. 298, p. 1407–1410.

Etheridge, M.A., Wall, V.J., Cox, S.F., and Vernon, R.H., 1984, High fluid pressures during regional metamorphism and deformation: Implications for mass transport and deformation mechanisms: Journal of Geophysical Research, v. 89, p. 4344–4358.

Ferry, J.M., 1994, A historical view of metamorphic fluid flow: Journal of Geophysical Research, v. 99, p. 15,487–15,498.

Jamtveit, B., Austrheim, H., and Malthe-Sorenssen, A., 2000, Accelerated hydration of the Earth's deep crust induced by stress perturbations: Nature, v. 408, p. 75–78.

Jiao, W.J., Silver, P.G., Fei, Y.W., and Prewitt, C.T., 2000, Do intermediate- and deep-focus earthquakes occur on preexisting weak zones? An examination of the Tonga subduction zone: Journal of Geophysical Research, v. 105, p. 28,125–28,138.

Kirby, S.H., Engdahl, E.R., and Denlinger, R., 1996, Intraslab earthquakes and arc volcanism: Dual physical expressions of crustal and uppermost mantle metamorphism in subducting slabs, *in* Bebout, G.E., et al., eds., Subduction: Top to bottom: American Geophysical Union Geophysical Monograph 96, p. 195–214.

Ko, S.C., Olgaard, D.L., and Wong, T.F., 1997, Generation and maintenance of pore pressure excess in a dehydrating system: 1. Experimental and microstructural observations: Journal of Geophysical Research, v. 102, p. 825–839.

Manning, C.E., and Ingebritsen, S.E., 1999, Permeability of the continental crust: Implications of geothermal data and metamorphic systems: Reviews of Geophysics, v. 37, p. 127–150.

McCulloch, M.T., and Woodhead, J.D., 1993, Lead isotopic evidence for deep crustal-scale fluid transport during granite petrogenesis: Geochimica et Cosmochimica Acta, v. 57, p. 659–674.

Meade, C., and Jeanloz, R., 1991, Deep-focus earthquakes and recycling of water into the Earth's mantle: Science, v. 252, p. 68–72.

Miller, S.A., van der Zee, W., Olgaard, D.L., and Connolly, J.A.D., 2003, A fluid-pressure feedback model of dehydration reactions: Experiments, modelling, and application to subduction zones: Tectonophysics (in press).

Murrell, S.A.F., and Ismail, I.A.H., 1976, The effect of decomposition of hydrous minerals on the mechanical properties of rocks at high pressures and temperatures: Tectonophysics, v. 31, p. 207–258.

Peacock, S.M., 2001, Are the lower planes of double seismic zones caused by serpentine dehydration in subducting oceanic mantle?: Geology, v. 29, p. 299–302.

Raleigh, C.B., and Paterson, M.S., 1965, Experimental deformation of serpentinite and its tectonic implications: Journal of Geophysical Research, v. 70, p. 3965–3985.

Roering, C., van Reenen, D.D., Smit, C.A., and Dutoit, R., 1995, Deep-crustal embrittlement and fluid-flow during granulite metamorphism in the Limpopo belt, South Africa: Journal of Geology, v. 103, p. 673–686.

Trommsdorff, V., and Evans, B.W., 1977, Antigorite-ophicarbonates: Phase relations in a portion of the system CaO-MgO-SiO_2-H_2O-CO_2: Contributions to Mineralogy and Petrology, v. 60, p. 39–56.

Ulmer, P., 2001, Partial melting in the mantle wedge—The role of H_2O in the genesis of mantle-derived ''arc-related'' magmas: Physics of the Earth and Planetary Interiors, v. 127, p. 215–232.

Ulmer, P., and Trommsdorff, V., 1995, Serpentine stability to mantle depths and subduction-related magmatism: Science, v. 268, p. 858–861.

Wong, T.F., Ko, S.C., and Olgaard, D.L., 1997, Generation and maintenance of pore pressure excess in a dehydrating system: 2. Theoretical analysis: Journal of Geophysical Research—Solid Earth, v. 102, p. 841–852.

Zhang, S., Cox, S.F., and Paterson, M.S., 1994, The influence of room-temperature deformation on porosity and permeability in calcite aggregates: Journal of Geophysical Research—Solid Earth, v. 99, p. 15,761–15,775.

Zhang, S., FitzGerald, J.D., and Cox, S.F., 2000, Reaction-enhanced permeability during decarbonation of calcite plus quartz → wollastonite plus carbon dioxide: Geology, v. 28, p. 911–914.

Zharikov, A.V., Lebedev, E.B., Dorfman, A.M., and Vitovtova, V.M., 2000, Effect of saturating fluid composition on the rock microstructure, porosity, permeability and Vp under high pressure and temperature: Physics and Chemistry of the Earth, v. 25, p. 215–218.

Manuscript received 7 April 2003
Revised manuscript received 26 June 2003
Manuscript accepted 8 July 2003

Printed in USA